Electrochemical etching of lightweight nanotips for high quality-factor quartz tuning fork force sensor: atomic force microscopy applications

Danish Hussain[1,2], Jianmin Song[1], Hao Zhang[1], Xianghe Meng[1], Hui Xie[1] ✉

[1]*State Key Laboratory of Robotics and Systems, Harbin Institute of Technology, Harbin 150080, People's Republic of China*
[2]*Department of Mechatronics Engineering, College of Electrical & Mechanical Engineering, National University of Sciences and Technology, Islamabad 44000, Pakistan*
✉ *E-mail: xiehui@hit.edu.cn*

Published in Micro & Nano Letters; Received on 30th December 2017; Revised on 16th April 2018; Accepted on 25th April 2018

Commercially available quartz tuning forks (QTFs) can be transformed into self-sensing and actuating force sensors by micro-assembling a sharp tip on the apex of a tine. Mass of the tip is critical in determining the quality (Q)-factor of the sensor, therefore, fabrication of the lightweight nanotips is a precondition for high Q-factor QTF sensors. The work reports fabrication of very lightweight tungsten nanotips with a two-step electrochemical etching technique which can be used to develop high Q-factor QTF force sensor. First, a tungsten wire with protective coating at one end (1–2 mm) is etched with a trapezoidal waveform to form a lengthy (~2–5 mm) and slender (diameter ~10–40 μm) micro-needle. In the second step, sharp tip apex is fabricated with a direct current etching. High Q-factor (6600–8000) QTF force sensors have been developed with the fabricated nanotips. Atomic force microscope scanning of nano-grating and a triblock copolymer surface validates the scanning performance of the developed sensors.

1. Introduction: Quartz tuning forks (QTFs) are used as versatile sensors in different sensing applications [1–3]. As force sensors they are used for atomic and subatomic level imaging, bio-molecular imaging and micro-/nano-manipulation [4–7]. A force sensor is fabricated by microassembling a sharp tip to a tine of the QTF. For a QTF with strictly symmetrical tines, the base does not have motion parallel to the tine's motion thus the energy dissipation due to the base vibration is minimised which leads to a higher quality(Q)-factor [8]. However, the attached tip breaks this symmetry and excites the base which results in the Q-factor degradation due to the energy dissipation through the base [8–10]. With the increasing tip mass the degradation in Q-factor is more pronounced therefore low mass of the tip is desired for achieving high Q-factor [11, 12]. On the other hand, higher Q-factor will lead to the higher force gradient sensitivity, as the minimum detectable force gradient is proportional to $1/\sqrt{Q}$ [13].

For sensor fabrication a nanotip is attached to the apex of a tine of the QTF and nanotips are usually fabricated by electrochemical etching of metallic wires, e.g. Pr-Ir [14], iron-based alloys [15], platinum [16], gold [17], rhodium, palladium [18], silver [19], copper, nickel [20] and tungsten [21, 22]. Several properties such as high mechanical strength, durability, high conductivity (for scanning tunnelling, field-ion microscopy and Kelvin probe microscopy) and reliability are important for the nanotips. Tungsten has high mechanical strength, low cost and its electrochemical etching is straightforward, therefore, it is widely used for tip fabrication [23–30].

Tungsten nanotips are commonly fabricated with the DC drop-off [14, 31], reverse electrochemical [32, 33] and dynamic etching techniques [34, 35]. Various DC drop-off methods have been used to fabricate very sharp nanotips [28, 29, 31]. However, shaft size of the DC etched nanotips is large and massive. On the other hand, several dynamic etching techniques are explored [21–25]. Ju *et al.* [24] proposed a method to dynamically control the neck-in position of a tungsten wire to fabricate nanotips with desirable lengths. Chang *et al.* [25] used an initial DC etching potential followed by a pulse etching to produce lengthy and sharp nanotips. Sharp nanotips can be fabricated by a reverse electrochemical etching technique [32, 33, 36] and by applying a voltage with optimised wave shape, phase angle and frequency [35]. Sharp tips with controlled profiles have been a prime focus of the previous researches and the tips fabricated with the above methods are normally massive which may lower the Q-factor. Therefore, new techniques for the fabrication of lightweight nanotips are indispensable to develop high Q-factor QTF force sensors.

In this work, we demonstrate a straightforward, two-step electrochemical etching process to fabricate lightweight and sharp nanotips for preparation of high Q-factor QTF sensors. First, one end of the wire is coated and etched with a trapezoidal signal. The coating hinders the effect of the fast etching at the lower end [21], thus the wire between air–electrolyte interface and coated region is etched into a long slender micro-needle. In the second step, the wire is elevated to a suitable height using a precision microstage of the custom designed etching setup and DC etching is performed to form a very sharp tip apex. With this method sharp and lightweight nanotips are fabricated with a high success rate. A home-built dual end-effector micromanipulator system is used to microassemble the fabricated nanotips on a tine of the QTF to develop high Q-factor self-sensing and actuating force sensors. Atomic force microscopy (AFM) scanning of TG1 (AFM grating) and ultra-precision micro-machined silicon surface performed with the nanotips.

2. Two-step etching method: Fig. 1 shows the electrochemical etching setup that is composed of a potassium hydroxide (KOH) solution container, stainless steel electrodes (L-shaped), a charge coupled device (CCD) camera, a wire holder (a commercial 0.1 mm pin hole drilling reamer chuck clamp), an oscilloscope (Agilent InfiniiVision DSO-X4024A) with integrated function generators and a DC voltage source. The wire holder is mounted on an *XYZ* microstage (MS I) to precisely control the tip submersion depth. CCD and KOH containers are mounted on individual microstages for camera course positioning and mobility of the KOH container. Steel electrodes are placed at a suitable distance apart from anode to avoid the disturbance at meniscus due to gas bubbles and retain uniform electrochemical forces on the anode.

As shown in Fig. 1 inset (i), one end coated (polyester enamel paint ~1–2 mm) polycrystalline tungsten (W) wire (diameter: 100 or 200 μm, length: 20–30 mm) is inserted into the holder and W

doi: 10.1049/mnl.2017.0924

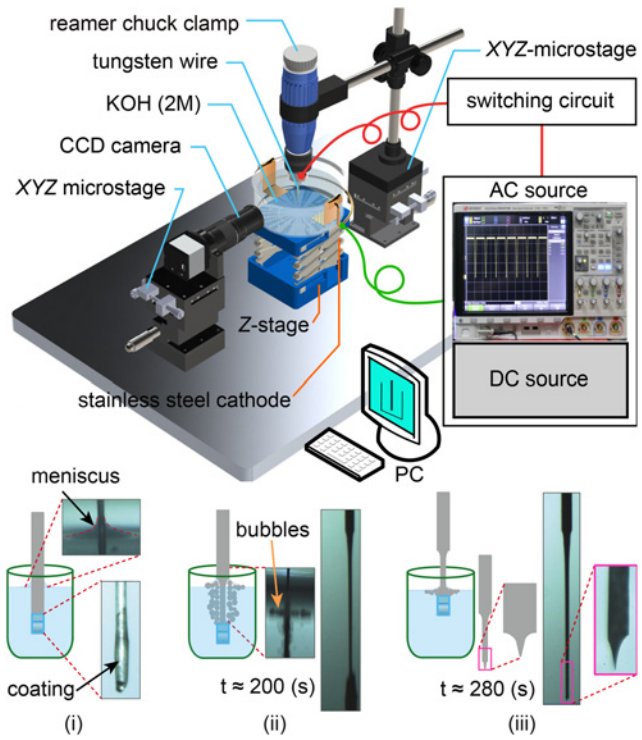

Fig. 1 *Schematic diagram showing two-step etching setup. Insets show corresponding tip profile evolution: (i) submerged tungsten wire with enamel coating at the end (1–2 mm); (ii) step-I: etching with the trapezoidal potential and micro-needle formed; (iii) step-II: DC etching and tip formed after the etching*

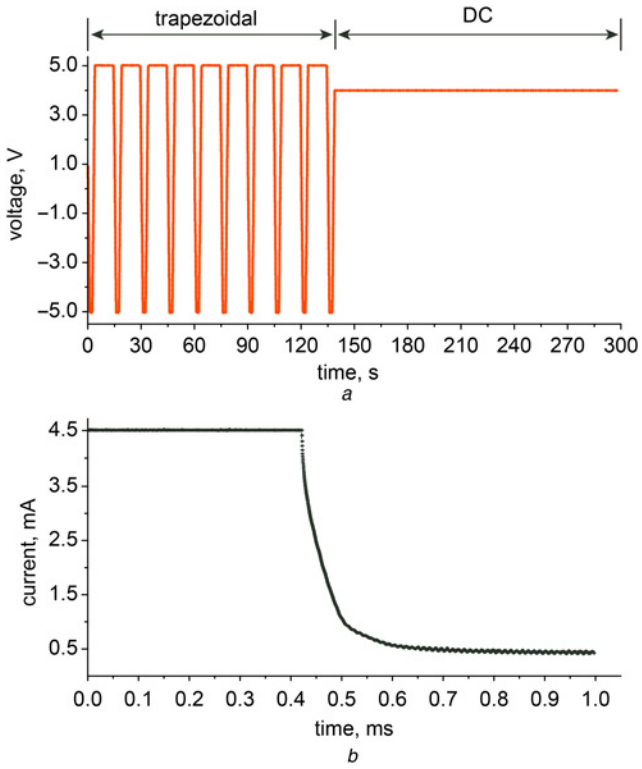

Fig. 2 *Etching waveform and DC etching current*
a Schematic diagram of the etching waveform used for the fabrication of light nanotips for high Q-factor tuning fork sensor. Left: trapezoidal signal, right: DC potential
b DC etching current as function of time

wire (6–8 mm) is submersed in the KOH solution using MS I. As shown in Fig. 1 inset (ii), tungsten (W) wire is first etched with a trapezoidal signal (Fig. 2*a* – left part) that is generated by the function generator of the Agilent oscilloscope (frequency: 20 Hz, voltage: 5 V peak-peak). AC etching is carefully monitored and stopped, when the wire diameter reduces enough (10–40 µm usually). In the conventional AC etching technique, the etching rate is higher at the lower end due to strong local electric field at the sharp geometries [14] and nanotips occasionally get blunt [20]. Therefore, they are less favourable for the QTF sensor development. In the proposed method, the coating is used to control the etching rate at the lower end, therefore, the middle portion of the tungsten wire between the meniscus and coating is etched into a cylindrical micro-needle with a neck near the meniscus. Etching time for the first step is not universal and it depends on the wire diameter, immersion depth, electrolyte concentration and signal shape, frequency as well as amplitude. Using 2 M KOH solution, 6–8 mm immersion depth and 5 V trapezoidal potential, time required for the first step is about 60 and ~200 s for wires with diameters of 100 and 200 µm, respectively.

In the second step, partially etched tungsten wire is elevated using MS I until the coating is near the air–electrolyte interface and etched with a DC potential (4–8 V). The motion resolution of the MS I is in sub-micrometre range therefore the submersion depth can be controlled very precisely. During the DC etching, most of the reaction occurs at the air–electrolyte interface. In contrast to the AC etching, in DC etching tungstate anions slide

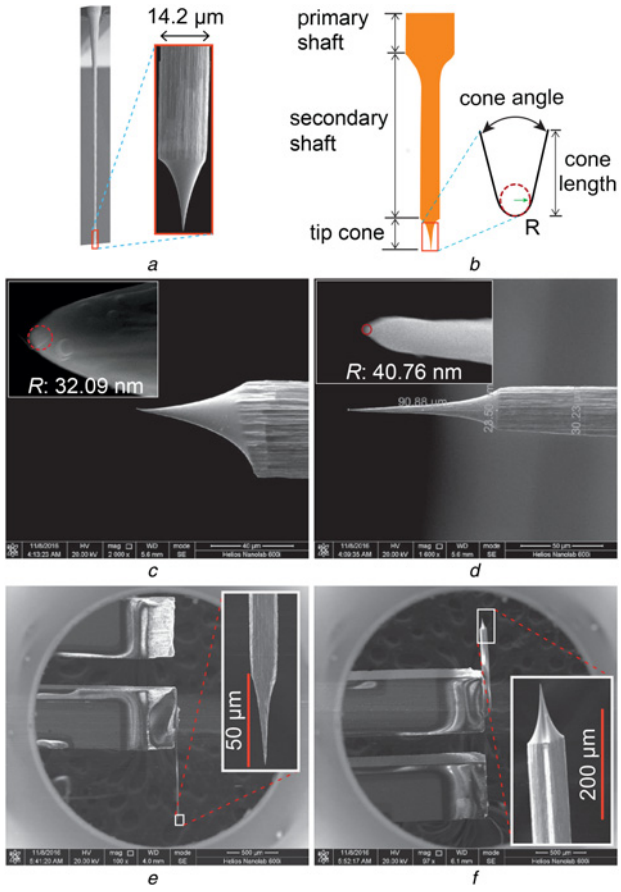

Fig. 3 *Schematic diagram and SEM images of two-step etched tips*
a SEM image
b Schematic diagram showing parameters of two-step etched tip, *R* is radius of curvature
c, *d* High-resolution SEM images of the two-step etched nanotips. Insets: close-up views of the tip apexes
e, *f* SEM images of the fabricated high Q-factor QTF sensors.

Table 1 Comparison of the sensors prepared by attaching nanotips fabricated by different etching techniques

Sensor	Method	f_{bare}, kHz	f_{sensor}, kHz	Q_{bare}	Q_{sensor}	Tip shaft length, μm	Tip shaft diameter, μm	Cone length, μm	R, nm
1	DC	32.771	31.356	13,119	600	646.88	100.00	94.59	33
2	DC	32.782	30.002	12,878	200	1228.3	100.00	130.12	41.6
3	AC	32.770	31.005	13,119	300	500.5	100.00	500.31	130
4	two-step	32.808	32.528	10,592	7980	1110.2	14.65	34.12	29.14
5	two-step	32.742	32.263	12,581	6662	1136.1	38.51	82.80	40
6	two-step	32.758	32.356	11,022	7636	1201.3	16.32	36.48	32.1

downwards along the wire surface and a subsequent inflow of electrolyte containing hydroxide (OH^-) ions occurs at this region. The downward flow of the tungstate anions form a dense layer at the portion lower than the meniscus which slows down the hydroxide ion activity at the lower portion of the wire [24, 33]. As a result, a neck is formed at the portion having higher reaction rate (i.e. at the meniscus region). After sufficient etching the neck becomes very thin and the coated part drops-off, leaving a tip with a sharp apex, as shown in Fig. 1 inset (iii). After sufficient etching the neck becomes very thin and the coated part is dropped-off thus leaving a sharp tip apex. Fig. 2*b* shows the etching current as a function of the etching time. At the time of the drop-off, etching current decreases very rapidly. Soon after etching, the nanotips are reined with ethanol and deionised water, and characterised with optical microscope and scanning electron microscope (SEM) imaging.

3. Results and discussion: Fig. 3*a* shows an SEM image of a two-step etched tip which has primary and secondary shafts wherein the former is the actual diameter of the wire (Fig. 3*b*). During the first step, the secondary shaft is formed with the diameter and length in ranges of 10–40 and 2–5 mm, respectively. Figs. 3*c* and *d* show high-resolution SEM images of the nanotips and insets show close-up views of the tip apexes fabricated in the second step. Light nanotips with radius of curvature (R) < 50 nm, cone length in range of 30–150 μm and aspect ratio of 2:1–3:1 can be produced with high yield rate.

Force sensors were fabricated using one type of commercial QTF. Its tines' length, thickness and width were measured as 3.85, 0.550 and 0.3 mm, respectively. Q-factor for the bare QTFs in air was measured with the nanonis commercial electronics (SPECS Zurich GmbH) in the range of 1000–14,000. QTFs with higher Q-factor were used for sensor fabrication. To prepare a QTF sensor, precision micromanipulation method is used to assemble the tip (with secondary shaft) on the QTF with a dual-manipulator system. Using manipulator I, small amount of glue (UV8023) is deposited on a tine of the QTF (fixed on the sample platform), and then the tip placed on the manipulator II is approached near the tine until the tip base is fully in contact with the QTF and glue is cured with ultraviolet light exposure. The assembly process is monitored via an optical microscope. Fig. 3*e* shows a SEM image of a fabricated QTF sensor with a slender tip, while Fig. 3*e* with a stumpy tip. It is demonstrated that the tip mass can be well controlled to achieve higher Q-factor.

To compare the Q-factor, sensors were developed by microassembling nanotips fabricated with different etching techniques. Q-factor and resonance frequency of the sensors are measured with Nanonis electronics (SPECS Zurich GmbH). Six sensors are shown in Table 1; the Q-factor of the sensors with the DC and AC etched nanotips is reduced greatly as compared to the Q-factor of the bare QTFs which is because of the massive tips. While the sensors prepared with the two-step etched nanotips show high Q-factor. For example, as shown in Fig. 4, Q-factor of the sensor-4 is measured as 7980 with only 25% reduction as compared to the bare QTF, which is a significant improvement in comparison to the previous results (<5000) [37] without using mass rebalancing or Q-control techniques [38, 39]. Similarly,

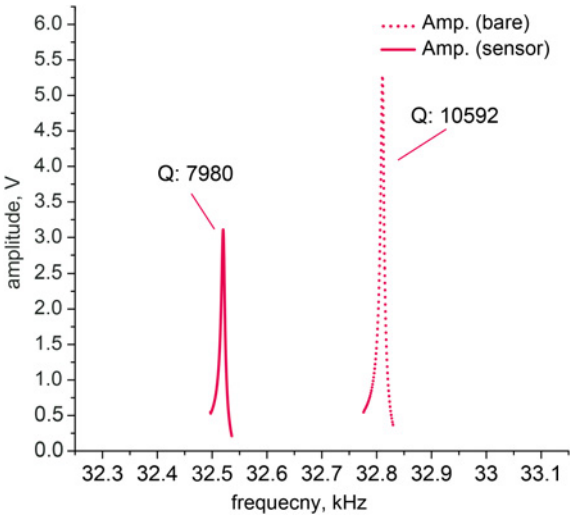

Fig. 4 *Frequency spectrum of the bare QTF and the prepared high Q-factor sensor-4. The excitation voltage was 12 mV (amplitude) sinusoidal waveform from OC4 (SPECS Zurich GmbH)*

attaching lightweight nanotips can significantly increase the Q-factor of qPlus sensor as well [40]. As in the mass re-balancing method, a counter mass equal to the tip mass should be attached on the opposite tine at the right location. In addition, the mass of the tip should be less than the tine's mass (lightweight) to recover Q-factor significantly, after mass rebalance [12]. Therefore, fabrication of the lightweight tips is highly important for mass rebalance method as well.

To show the scanning capability of the nanotips, two samples were imaged in force modulation mode with the fabricated sensor-4 using a home-built AFM [41]. An AFM calibration grating (TGZ1) (NT-MDT Russia) with nominal period and height of 3 ± 0.01 μm and 21.6 ± 1.5 nm was first scanned. Figs. 5*a* and *b* show grating surface topography and height profile, respectively. For measuring period and step height of the grating, ten line profiles across the grating were extracted at equal intervals along the grating. The averaged period and step height are 3.02 μm and 22 nm, respectively, which are in good agreement with the nominal values. In addition, triblock copolymer poly-styrene-block-poly(ethylene/butylene)-block-polystyrene (SEBS) thin film was scanned to demonstrate the spatial resolution of the proposed the QTF sensor. As shown in Fig. 6*a*, the SEBS copolymer surface is formed with ordered structures, and the cross-section profile (Fig. 6*b*) indicates that the average height of the cylindrical patterns was ~8–15 nm and exhibited a high lateral resolution which could be further improved by using a sharper tip.

In this work, lightweight nanotips are fabricated with a proposed two-step electrochemical etching method. The fabricated nanotips were microassembled on the QTF using a home-made dual end-effector micro-manipulation system. The sensors developed with the two-step etched nanotips have shown high Q-factor due to their lightweight. SEM characterisation shows that the nanotips

doi: 10.1049/mnl.2017.0924

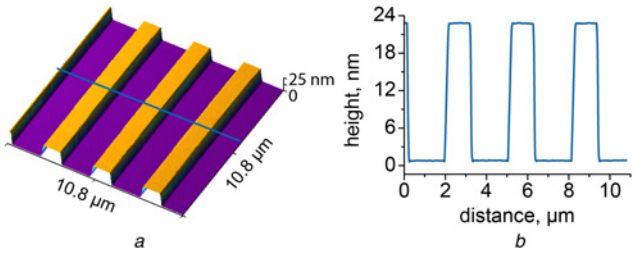

Fig. 5 *Scanning of the AFM calibration grating*
a AFM topography of TGZ1
b Height profile. Image resolution: 240 × 240 pixels

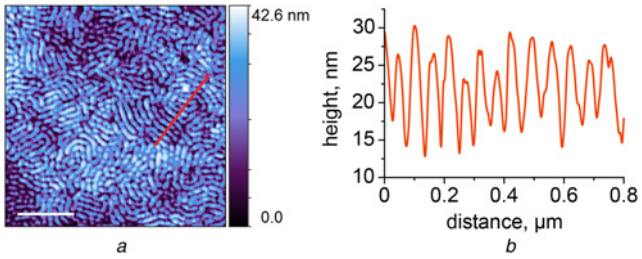

Fig. 6 *High spatial resolution scanning of a SEBS polymer surface*
a Topography
b Line profile. Scale bars, 500 nm

have comparable sharpness with the DC etched tips which is further validated by the high-resolution AFM imaging of a triblock copolymer surface. Moreover, fabricated high Q-factor QTF sensors can be used in several AFM applications such as bio-manipulation, bio-mechanics and nanometrology. Furthermore, it can be used for critical dimension metrology of microstructures by replacing optical lever based tilted sensor [42] with a tilted QTF sensor in the future work.

4. Conclusion: We report fabrication of lightweight tungsten nanotips with a simple and straightforward two-step electrochemical etching technique. Slender and sharp nanotips with primary shaft diameter and length in the range of 10–40 μm and 2–5 mm, respectively, can be fabricated with high success rate (~80%). QTF sensors developed with the fabricated nanotips show high Q-factor in the range of 6600–8000 which is a significant improvement without using balancing or Q-control techniques. In addition, such lightweight tips are also important for high Q-factor achievement after mass rebalance as the mass of the tip should be less than the mass of a tine for Q-factor recovery after mass rebalance. Finally, the high-resolution AFM images of triblock copolymer surface and AFM grating validate the performance of the sensor.

5. Acknowledgment: This work was supported by the National Natural Science Foundation of China under grant nos. 61573121 and 51521003, State Laboratory of Robotics and Systems under grant no. SKLRS201619B. Danish Hussain acknowledges the support of Higher Education Commission of Pakistan for his studies in China.

6 References

[1] Li C., Zhao Y., Cheng R., *ET AL.*: 'Microresonant accelerometer composed of silicon substrate and quartz double-ended tuning fork with temperature isolator', *Micro Nano Lett.*, 2016, **11**, (7), pp. 382–385
[2] Liang J., Chai Y., Meng G., *ET AL.*: 'Surface electrode configurations for quartz MEMS double-ended tuning fork resonator', *Micro Nano Lett.*, 2013, **8**, (1), pp. 52–55
[3] Kosterev A.A., Tittel F.K., Serebryakov D.V., *ET AL.*: 'Applications of quartz tuning forks in spectroscopic gas sensing', *Rev. Sci. Instrum.*, 2005, **76**, (4), p. 043105
[4] Makky A., Viel P., Chen S.W.W., *ET AL.*: 'Piezoelectric tuning fork probe for atomic force microscopy imaging and specific recognition force spectroscopy of an enzyme and its ligand', *J. Mol. Recognit.*, 2013, **26**, (11), pp. 521–531
[5] Acosta J.C., Hwang G., Polesel-Maris J., *ET AL.*: 'A tuning fork based wide range mechanical characterization tool with nanorobotic manipulators inside a scanning electron microscope', *Rev. Sci. Instrum.*, 2011, **82**, (3), p. 035116
[6] Rensen W.H.J., Van Hulst N.F., Ruiter A.G.T., *ET AL.*: 'Atomic steps with tuning-fork-based noncontact atomic force microscopy', *App. Phy. Lett.*, 1999, **75**, (11), pp. 1640–1642
[7] Giessibl F.J., Hembacher S., Bielefeldt H., *ET AL.*: 'Subatomic features on the silicon (111)-(7 × 7) surface observed by atomic force microscopy', *Science*, 2000, **289**, (5478), pp. 422–425
[8] Naber A.: 'The tuning fork as sensor for dynamic force distance control in scanning near-field optical microscopy', *J. Microsc.*, 1999, **194**, pp. 307–310
[9] Shelimov K.B., Davydov D.N., Moskovits M.: 'Dynamics of a piezoelectric tuning fork/optical fiber assembly in a near-field scanning optical microscope', *Rev. Sci. Instrum.*, 2000, **71**, (2), p. 437
[10] Castellanos-Gomez A., Agraït N., Rubio-Bollinger G.: 'Dynamics of quartz tuning fork force sensors used in scanning probe microscopy', *Nanotechnology*, 2009, **20**, (21), p. 215502
[11] Smit R.H., Grande R., Lasanta B., *ET AL.*: 'A low temperature scanning tunneling microscope for electronic and force spectroscopy', *Rev. Sci. Instrum.*, 2007, **78**, p. 113705
[12] Hussain D., Song J., Zhang H., *ET AL.*: 'Optimizing the quality factor of quartz tuning fork force sensor for atomic force microscopy: impact of additional mass and mass rebalance', *IEEE Sen. J.*, 2017, **17**, (9), pp. 2797–2806
[13] Martin Y., Williams C.C., Wickramasinghe H.K.: 'Atomic force microscope-force mapping and profiling on a sub 100-Å scale', *J. App. Phy.*, 1987, **61**, (10), pp. 4723–4729
[14] Klein M., Schwitzgebel G.: 'An improved lamellae drop-off technique for sharp tip preparation in scanning tunneling microscopy', *Rev. Sci. Instrum.*, 1997, **68**, (8), pp. 3099–3103
[15] Kim Y.C., Yu C.J., Seidman D.N.: 'Effects of low-energy (1–1.5 kV) nitrogen-ion bombardment on sharply pointed tips: sputtering, implantation, and metal-nitride formation', *J. App. Phy.*, 1997, **81**, (2), pp. 944–950
[16] Libioulle L., Houbion Y., Gilles J.M.: 'Very sharp gold and platinum tips to modify gold surfaces in scanning tunneling microscopy', *J. Vac. Sci. Technol. B*, 1995, **13**, (3), pp. 1325–1331
[17] Boyle M.G., Feng L., Dawson P.: 'Safe fabrication of sharp gold tips for light emission in scanning tunnelling microscopy', *Ultramicroscopy*, 2008, **108**, pp. 558–566
[18] Nam A.J., Teren A., Lusby T.A., *ET AL.*: 'Benign making of sharp tips for STM and FIM: Pt, Ir, Au, Pd, and Rh', *J. Vac. Sci. Technol. B*, 1995, **13**, (4), pp. 1556–1559
[19] Gorbunov A.A., Wolf B., Edelmann J.: 'The use of silver tips in scanning tunneling microscopy', *Rev. Sci. Instrum.*, 1993, **64**, (1), pp. 2393–2394
[20] Lemke H., Göddenhenrich T., Bochem H.P., *ET AL.*: 'Improved microtips for scanning probe microscopy', *Rev. Sci. Instrum.*, 1990, **61**, (10), pp. 2538–2541
[21] Valencia V.A., Thaker A.A., Derouin J., *ET AL.*: 'Preparation of scanning tunneling microscopy tips using pulsed alternating current etching', *J. Vac. Sci. Technol. A.*, 2015, **33**, (2), p. 023001
[22] Hobara R., Yoshimoto S., Hasegawa S., *ET AL.*: 'Dynamic electrochemical-etching technique for tungsten tips suitable for multi-tip scanning tunneling microscopes', *e-J. Surf. Sci. Nanotech.*, 2007, **5**, pp. 94–98
[23] Toh S.L., Tan H., Lam J.C., *ET AL.*: 'Optimization of AC electrochemical etching for fabricating tungsten nanotips with controlled tip profile', *J. Electrochem. Soc.*, 2010, **157**, (1), pp. E6–E11
[24] Ju B.F., Chen Y.L., Yaozheng Ge Y.: 'The art of electrochemical etching for preparing tungsten probes with controllable tip profile and characteristic parameters', *Rev. Sci. Instrum.*, 2011, **82**, (1), p. 013707
[25] Chang W.T., Hwang S., Chang M.T., *ET AL.*: 'Method of electrochemical etching of tungsten tips with controllable profiles', *Rev. Sci. Instrum.*, 2012, **83**, (8), p. 083704
[26] Tahmasebipour G., Hojjat Y., Ahmadi V., *ET AL.*: 'Optimization of STM/FIM nanotip aspect ratio based on the Taguchi method', *Int. J. Adv. Manuf. Tech.*, 2009, **44**, (1–2), pp. 80–90

[27] Garnaes J., Kragh F., Mo K.A., *ET AL.*: 'Transmission electron microscopy of scanning tunneling tips', *J. Vac. Sci. Technol. A*, 1990, **8**, (1), pp. 441–444
[28] Anwei L., Xiaotang H., Wenhui L., *ET AL.*: 'An improved control technique for the electrochemical fabrication of scanning tunneling microscopy microtips', *Rev. Sci. Instrum.*, 1997, **68**, (10), pp. 3811–3813
[29] Bourque H., Leblanc R.M.: 'Electrochemical fabrication of scanning tunneling microscopy tips without an electronic shut-off control', *Rev. Sci. Instrum.*, 1995, **66**, (3), pp. 2695–2697
[30] Nave M., Rubin B., Maximov V., *ET AL.*: 'Transport-limited electrochemical formation of long nanosharp probes from tungsten', *Nanotech.*, 2013, **24**, p. 355702
[31] Oliva A.I., Romero G.A., Pena J.L., *ET AL.*: 'Electrochemical preparation of tungsten tips for a scanning tunneling microscope', *Rev. Sci. Instru.*, 1996, **67**, (5), pp. 1917–1921
[32] Kar A.K., Gangopadhyay S., Mathur B.K.: 'A reverse electrochemical floating-layer technique of SPM tip preparation', *Meas. Sci. Technol.*, 2000, **11**, (10), p. 1426
[33] Meza J.M., Polesel-Maris J., Lubin C., *ET AL.*: 'Reverse electrochemical etching method for fabricating ultra-sharp platinum/iridium tips for combined scanning tunneling microscope/atomic force microscope based on a quartz tuning fork', *Curr. Appl. Phys.*, 2015, **15**, (9), pp. 1015–1021
[34] Ju B.F., Chen Y.L., Fu M., *ET AL.*: 'Systematic study of electropolishing technique for improving the quality and production reproducibility of tungsten STM probe', *Sens. Actuators A, Phys.*, 2009, **155**, (1), pp. 136–144
[35] Lassner E., Schubert W.: 'Tungsten: properties, chemistry, technology of the element, alloys, and chemical compounds' (Springer, New York, 1999)
[36] Fotino M.: 'Nanotips by reverse electrochemical etching', *Appl. Phys. Lett.*, 1992, **60**, (23), pp. 2935–2937
[37] Kim K., Park J.Y., Kim K.B., *ET AL.*: 'Mechanically stable tuning fork sensor with high quality factor for the atomic force microscope', *Scanning*, 2014, **36**, (6), pp. 632–639
[38] Ng B.P., Zhang Y., Kok S.W., *ET AL.*: 'Improve performance of scanning probe microscopy by balancing tuning fork prongs', *Ultramicroscopy*, 2009, **109**, (4), pp. 291–295
[39] Jahng J., Lee M., Noh H., *ET AL.*: 'Active Q control in tuning-fork-based atomic force microscopy', *Appl. Phys. Lett.*, 2007, **91**, (2), p. 023103
[40] Labidi H., Kupsta M., Huff T., *ET AL.*: 'New fabrication technique for highly sensitive qPlus sensor with well-defined spring constant', *Ultramicroscopy*, 2015, **158**, pp. 33–37
[41] Xie H., Hussain D., Yang F., *ET AL.*: 'Development of three-dimensional atomic force microscope for sidewall structures imaging with controllable scanning density', *IEEE/ASME Trans. Mechatronics*, 2016, **21**, (1), pp. 316–328
[42] Xie H., Hussain D., Yang F., *ET AL.*: 'Atomic force microscopy deep trench and sidewall imaging with an optical fiber probe', *Rev. Sci. Instrum.*, 2014, **85**, (12), p. 123704

doi: 10.1049/mnl.2017.0924